

The Effect of Surroundings with Different Separation Distances on Surface Pressures on Low-Rise Buildings

Cheng-Hsin Chang¹ and Robert N. Meroney²

1) Department of Civil Engineering, Tamkang University, Taipei, Taiwan

2) WERFL, Department of Civil Engineering, Colorado State University, Fort Collins, CO 80523

ABSTRACT

Very large roof suctions on low-rise buildings occur for isolated buildings during both full-scale experiments and wind tunnel tests performed by many investigators. This paper investigates the sensitivity of these high suctions to the presence of multiple surrounding building configurations. This study uses as a basic building shape the Wind Engineering Research Field Laboratory building (WERFL) studied during the CSU/TTU Cooperative Program in Wind Engineering. A model of the WERFL structure was constructed to a 1:50 scale and instrumented with multiple pressure ports. Pressure taps on the 1:50 scale building model were connected to two 48-channel PSI transducer units. A large number of “dummy” models of similar dimensions were constructed to represent surrounding buildings. These model buildings were arranged in various symmetric configurations with different separation distances, and placed in the Industrial Wind Tunnel of the Wind Engineering and Fluids Laboratory, Colorado State University. Measurements include mean, rms and peak pressures, street canyon velocity profiles and laser-sheet flow visualizations. Shelter effects produced by the surrounding buildings on the central instrumented building were found to be significant, such that flow patterns are displaced and mean and peak induced loads are significantly different from the isolated building base case.

Key words: wind tunnel, wind load, shielding effect, urban street canyon, low-rise building

1. INTRODUCTION

The flow patterns that develop around individual buildings govern the wind forces on the building, the distribution of pressure about the building and scalar dispersion about the building and in its wake. The superposition and interaction of flow patterns associated with adjacent buildings govern the final distribution of facade pressures and the movement of pollutants in urban and industrial complexes. Street canyon depth and width, intersection locations, canyon orientation to dominate wind directions and building geometries will determine peak pollution incidents (Theurer [1]).

Many studies have shown that the worst mean and peak suctions on flat building roofs occur for cornering or oblique wind angles. At such angles, conical or delta wing vortices form along the roof edges, which induce higher suction pressures, associated with the strongly curved separation streamlines (Banks et al., [2] [3]). Yet the presence of nearby buildings is expected to deflect streamlines, modify local circulation patterns and induce modified patterns of suction and stagnation pressure, as well as different convection patterns for pollutants. Many studies have previously examined physical models of urban street canyons. Plate et al. [4] studied models of the development of the atmospheric boundary above urban areas by measuring flows over different

arrangements of buildings. Plate considered the effects of urban climates and urban climate modeling. Surry [5] examined the effect of both surroundings and roof corner geometric modifications on the roof pressures measured on a low-rise building. Kiefer and Plate [6] provided modeling of mean and fluctuation wind loads in different type of build-up areas. Most recently, Macdonald [7] modeled the mean velocity profiles in an urban canopy layer and examined the effect of a reduction of turbulence length scale with increasing obstacle-packing density.

Advanced technology makes computers faster and more powerful, which allows computational dynamics (CFD) procedures to be applied to many experimental flow problems. Today, increasing applications of CFD to wind engineering problems include wind load of building and pollutant dispersion phenomena. Several previous studies have compared measurements made during physical modeling with numerical predictions. He and Song [8] simulated the wind flow around the Texas Tech University (TTU) building and roof corner vortex by using a Large Eddy Simulation (LES) code. They claimed that the three-dimensional roof corner vortex pattern was successfully simulated and that mean values of pressure predicted were in good agreement with wind tunnel and field test measurements. Murakami et al [9] generated velocity fluctuations for an inflow boundary condition for the LES model with prescribed spatial correlation distributions and turbulence intensity levels. . Lee et al. [10] solved for wind effects on bluff bodies using the LES model and the finite element method, and they compared simulated results with numerical and experimental studies reported by other researchers. Selvam [11] used LES to compute the pressures around the TTU building using different inflow turbulence conditions, and he compared them with available field mean and peak pressure coefficients. Rehm et al. [12] compared mean surface pressures on a single building by using an LES algorithm with uniform and shear inflows. Cheatham et al [13] also simulated the flow and dispersion around a surface-mounded cube, and they examined the effect of resolution, boundary conditions, and the form of the inflow velocity profiles. Carpenter and Locke [14] investigated wind speeds over multiple two-dimensional hills and compared results with numerical solutions.

The goal of this paper is to investigate the bluff body flow and wind load in an idealized urban environment. Other companion papers report the impact of the same building geometries on point and line source diffusion over the building complex (Chang and Meroney, [15] [16]) The research consists of two components: physical urban street canyon fluid modeling in a boundary layer wind tunnel and numerical urban street canyon modeling using a finite-volume numerical method.

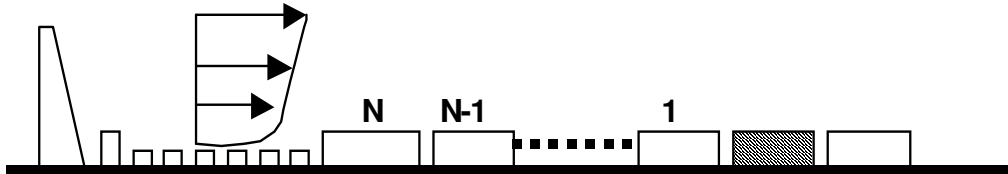
1.1 Fluid Modeling

This study uses a basic building shapesimilar to the Wind Engineering Research Field Laboratory building (WERFL) at Texas Tech University, Lubbock, which is a metal building of simple rectangular prism form (9.2 m x 13.8 m x 4.0 m tall) to build an urban street canyon model. Pressure fields, flow and dispersion patterns about this isolated building have been extensively measured both at full scale and over various model scales immersed in an equivalent turbulent shear layer (Cochran [17]; Birdsall [18]; Ham [19]; Banks [20]).

A plastic model of the WERFL structure was constructed to a 1:50 scale and instrumented with multiple pressure ports. A large number of “dummy” models of similar dimensions were constructed of plastic foam and wood to represent surrounding buildings. These buildings were arranged in various symmetric configurations with different separation distances in the Industrial

Wind Tunnel of the Wind Engineering and Fluid Laboratory, Colorado State University. Typical building patterns are noted in Figure 1, and the associated arrangement patterns are listed in Table 1.

{I RECCOMMEND YOU ADD AN EXPLANATION OF THE VARIABLE N AND MAYBE ANOTHER FIGURE AFTER FIGURE 1 TO EXPLAIN THE PRESENCE OF UPWIND BUILDINGS, THE UPWIND WINDTUNNEL CONFIGURATION OF SPIRES AND ROUGHNESS, THE VALUE OF THE POWERLAW & TURBULENT INTENSITY.



Wind velocity measurements are made with single hot-film probe and anemometry equipment manufactured by Thermo-Systems, Inc. (TSI). Flow visualization is accomplished with a laser-light sheet produced by 5-watt Coherent Innova 7005 Argon ion water-cooled laser. Images are recorded by using a Panasonic Omni vision II camera/recorder system. Pressure taps on the 1:50 scale building model are connected to a 48-channel Pressure System Inc. (PSI) “ESP48” transducer unit that is also mounted inside the model. Transducer voltages are integrated and recorded automatically by a National Instrument Inc. LabVIEW based data acquisition system.

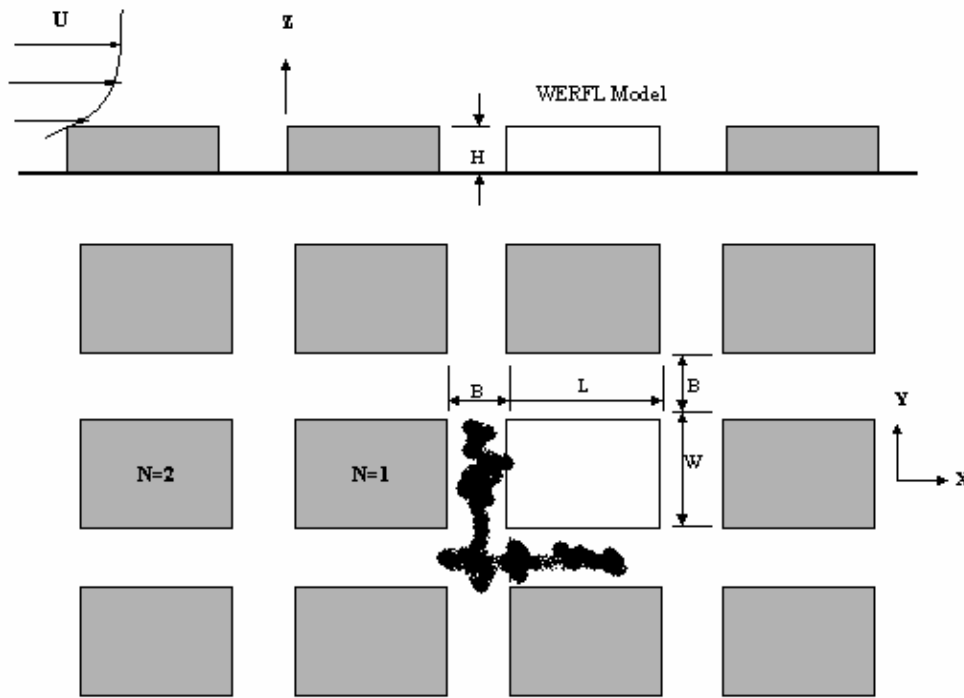


Figure 1: Schematic of Urban Street-canyon Model Arrangement

Add footnote to Flow column in table ie Flow*

B/H	λ_{area}	$\lambda_{\text{frontal area}}$	N rows	Structure	Flow
0.5	.72	.21	1,2,3,&8	City center	Skimming flow
1.0	.54	.16	1,2,3,&8	City center	Skimming flow
2.0	.34	.10	1,2,3,&8	Suburban	Wake interference
4.0	.17	.05	1,2,3,&8	Urban 1-2 stories	Wake interference
6.0	.10	.03	1,2,3,&8	One story houses	Isolated

$\lambda_{\text{area}} = \Sigma \text{ Areas covered by buildings} / \text{total urban area}$

$\lambda_{\text{frontal area}} = \Sigma \text{ Building area normal to wind} / \text{total urban area}$

* See Section 2 for definitions

Table 1: Array of model structures studied, $X_{\text{source}} = B/2$

1.2 Numerical Modeling

Flow over various building pattern arrangements are also simulated with the Fluent 5.4 computational fluid dynamics software.

The Fluent CFD software is based on a finite volume discretization of the equations of motion, an unstructured grid volume made of either rectangular prisms or tetrahedral cells, various matrix inverting routines, and, in this case, a kappa-epsilon (κ - ϵ) turbulence model. [21] Steady state solutions are sought for several flow configurations, and the data generated were displayed on various isopleth contour plots of velocity, turbulence and mean pressure coefficient. The effects of grid resolution, boundary conditions and selection of turbulence model were examined in a series of sensitivity calculations as reported by Chang [22]. [].

2. RESULTS AND DISCUSSION

As noted previously, multiple building configurations are considered. Depending on the street width to building height ratio (B/H), the flow in the street canyons can be classified as skimming flow (B/H=0-1.2), wake interference flow (B/H=1.2-5.0), or isolated roughness flow (B/H>5.0) as originally proposed by Oke [23]. Wind tunnel flow visualization results matched these proposed by Oke.

High suction pressures over the building surface are significantly reduced for a building surrounded by other buildings compared to the isolated building in the same approach flow, in terms of the peak, mean or RMS C_p . All three statistical interpretations of pressure variation are significantly reduced by the presence of surrounding buildings. See Figures 2 for detailed C_p comparisons on a single building and all surrounding cases.

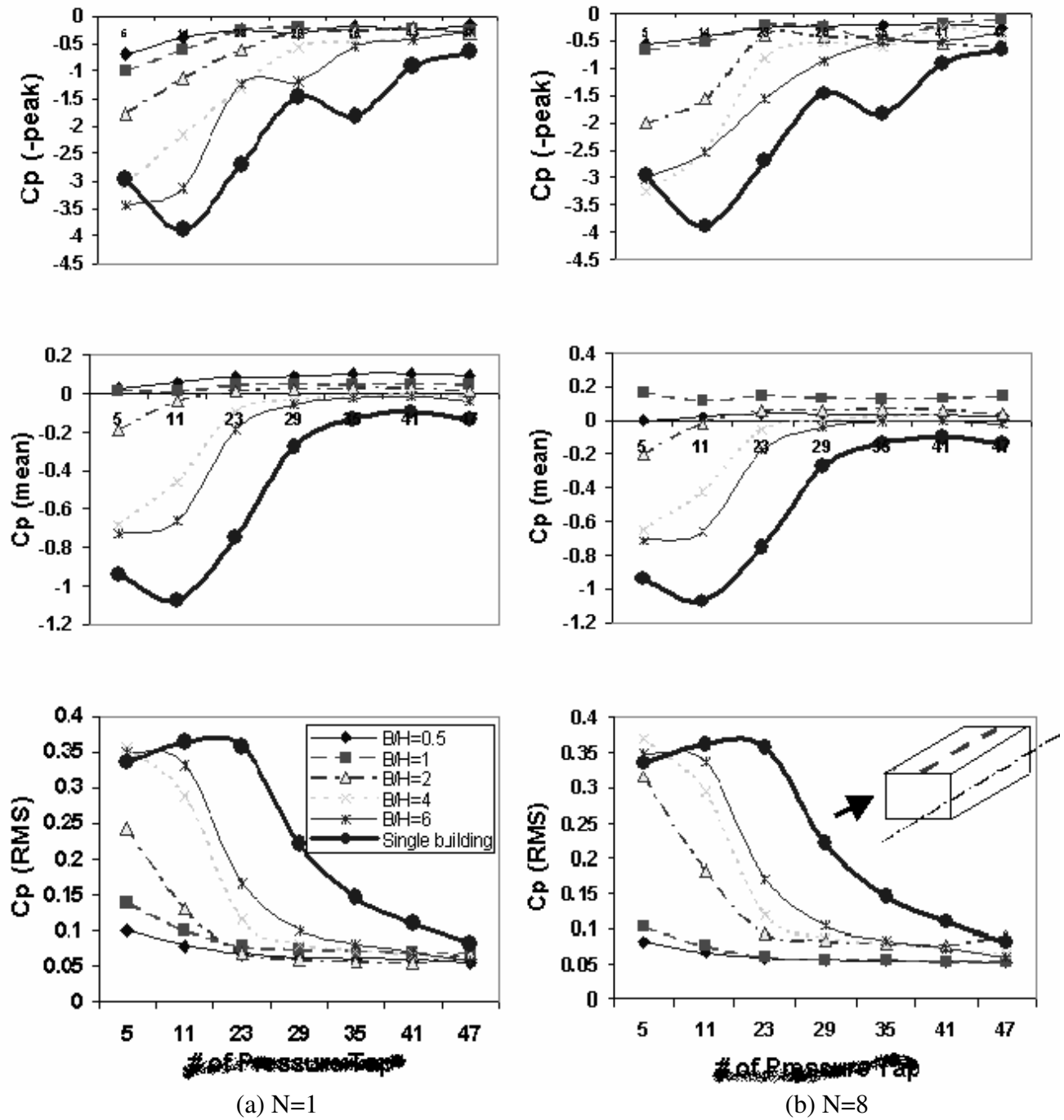
{ I am not happy about the next paragraphs, in trying to improve clarity I may have changed what you feel you observed. Read it over carefully before accepting my changes. }

It was expected that shielding effects depend on the width of the street canyon (ratio of B/H) and the number of the buildings located upstream of the master building. When examining the open-country cases (N=1) for different values of B/H and wind perpendicular to the building wall, the results show that as the value of B/H increases, the shielding effect on the roof C_p 's decrease. For example, the -mean, -peak and RMS C_p 's for the case of B/H=0.5 are all smaller than the case of

B/H=6. When one compare the open-country cases (N=1) and different values of B/H with the single building case, the -mean, -peak and RMS C_p 's reduce in all situations. However, in the upwind region of the roof along the centerline, RMS and peak $-C_p$'s are larger than those of the single building case due to flow separation occurring at the forward corner. The upwind wall cases have similar results to the roof cases. The shielding effects become larger with lower B/H (See Figures 2a).

For urban roughness cases (N=8), the shielding effects have similar trends to the open-country cases mentioned above. However, the shielding effects of the upwind buildings for the urban roughness cases are greater than for the open-country cases, because the effective boundary flow is displaced upward and a significant displacement thickness exists upwind of the master building (See Figures 2b).

Mean, RMS and -peak pressure coefficients measured in the wind tunnel for a corner roof point (Tap #1) for the wind azimuths range from 0 degree to 90 degrees are shown at Figures 3a, 3b and 3c. Pressure tap #1 corresponds to location of the tap 50101 as assigned to the measurements on the TTU/WERFL field building. This tap exhibited the highest suction pressures during the initial field study [15].



{ If possible revise the horizontal axis for the above figures to be distance from upwind leading edge of the building. }

Figure 2. Pressure coefficients (-peak, mean, and RMS) on the centerline of roof for cases, (a) N=1, (b) N=8 with different B/H

Figure 3d also shows a schematic for pressure coefficient measurement at different approach angles. For mean pressure coefficient, the results show that the maximum value of -1.8 occurs at the

wind angle of 10 degrees for the single building case. For other cases, the maximum mean C_p 's reduce to -0.3 , -0.7 and -0.5 for cases of $B/H=0.5$, $B/H=1$ and $B/H=2$, respectively. For RMS pressure coefficient, the result of the single building case shows that the maximum RMS C_p is 0.8 at the wind angle of 20° and 70° . Measurements and evaluation by Banks and Meroney [2] [3] relate the RMS maximums to instabilities in the twin vortex pairs originating at the upwind building corner. The values of RMS reduce to 0.1 , 0.3 and 0.35 for cases of $B/H=0.5$, $B/H=1$ and $B/H=2$, respectively. For $-$ peak pressure coefficient, the maximum value of the single building case is -4.1 at the wind angle of 10° . The maximum values of $-$ peak reduce to -0.8 , -1.6 and -1.5 for cases of $B/H=0.5$, $B/H=1$ and $B/H=2$, respectively. The case of $B/H=0.5$ has the maximum reduction rate for each pressure coefficient. The surrounding buildings shelter effects lead to a reduction in magnitude of 83% for the mean C_p , 87% for the RMS C_p and 80% for the $-$ peak C_p . High suction at the roof corner is significantly reduced when surrounding buildings are presented for all cases of wind flow angle varying from 0 to 90 degrees.

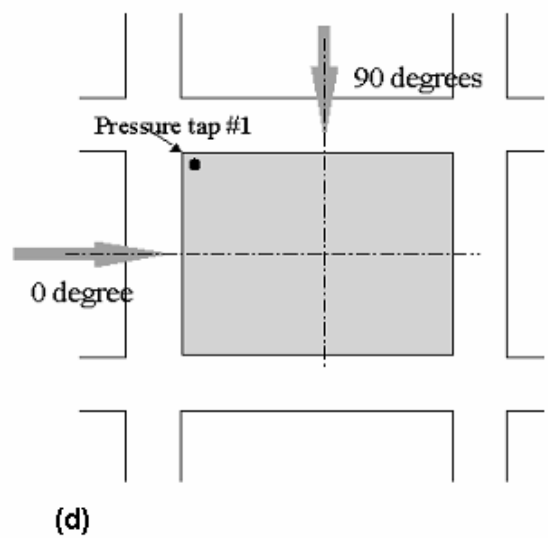
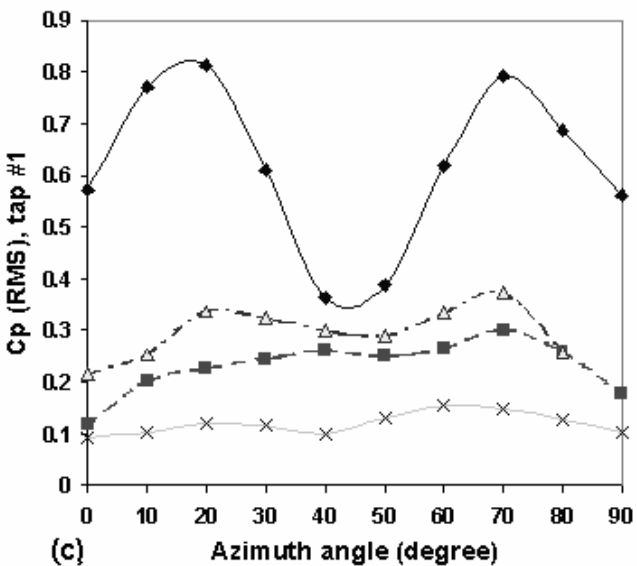
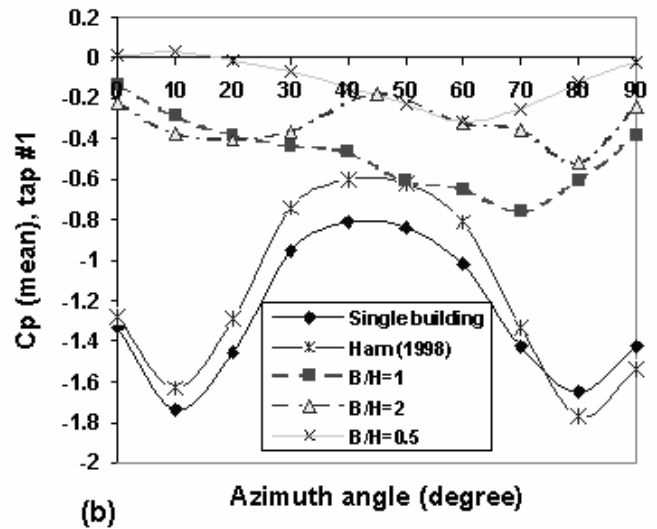
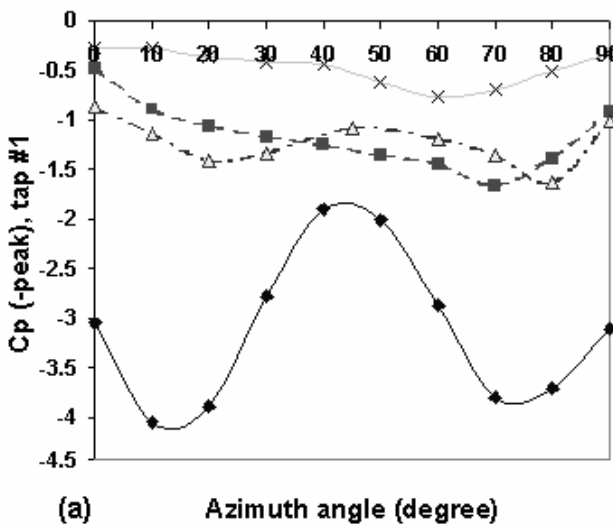


Figure 3 (a, b and c). - peak, mean and RMS pressure coefficient measurement for a roof corner point for the wind azimuths ranging from 0 to 90 degrees. (d) The schematic of pressure coefficient measurement in different approaching angles

3. COMPARISON OF WIND TUNNEL RESULTS AND NUMERICAL RESULTS

The pressure coefficients calculated by Fluent using the κ - ϵ turbulence model are compared to the wind tunnel results. Fluent was solved in a steady-state mode; hence, only the mean C_p can be determined since minimization of pressure deviations was used to produce solution convergence. Figure 4a compares mean wind pressure coefficients on the centerline of the roof of the master building with relevant results from numerical simulations carried out by using the Fluent κ - ϵ model. The graph shows both numerical data and experimental data of cases for different values of B/H . The symbols locate the experimental data and the different style lines follow the numerical data. The overall results appear similar to that of the experimental data with the exception of the front edge of the centerline region at flow separation in which case the numerical results indicate higher suction. Figure 4b shows comparisons of the mean C_p 's along the centerline of the downwind wall of the street canyon. The numerical results are similar to that of the experimental results, except that CFD predicts higher suction on the upper part of the centerline of the downwind wall of the street canyon.

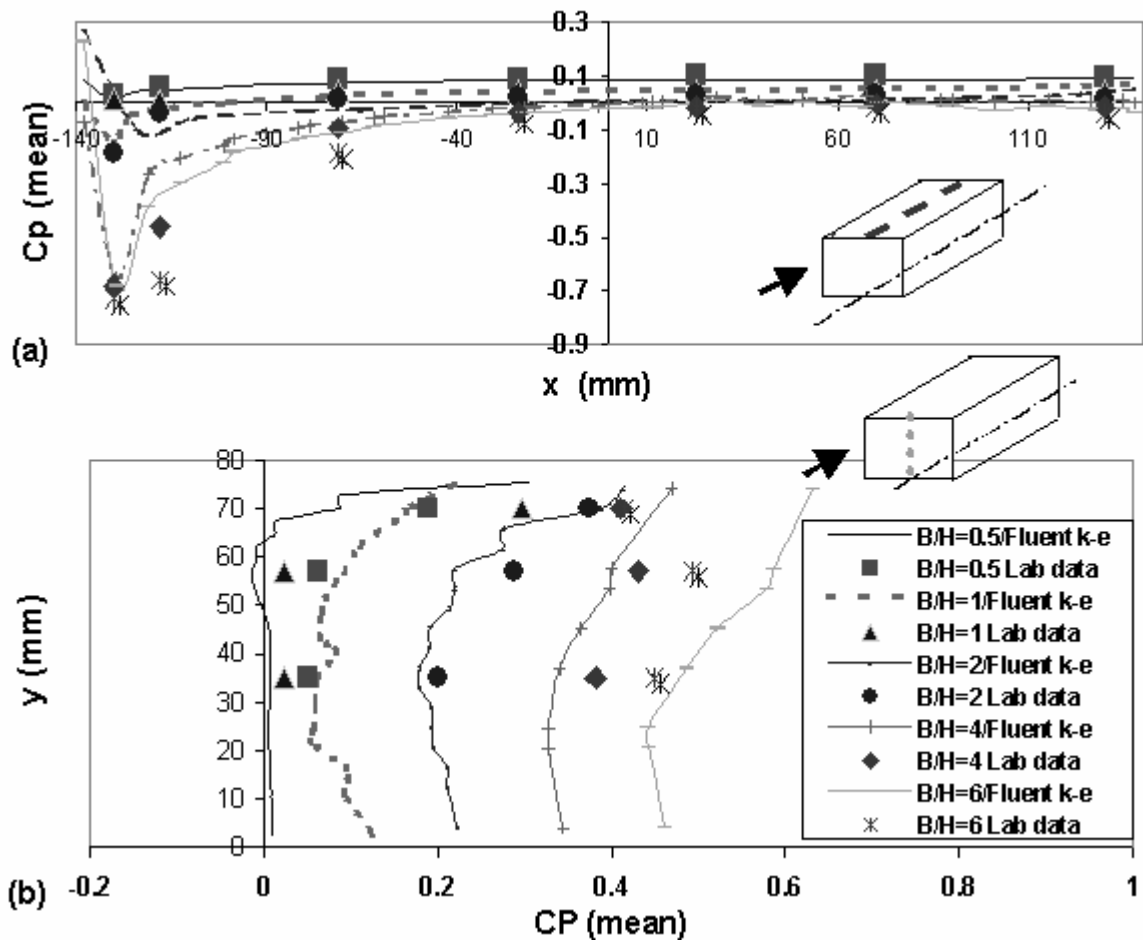


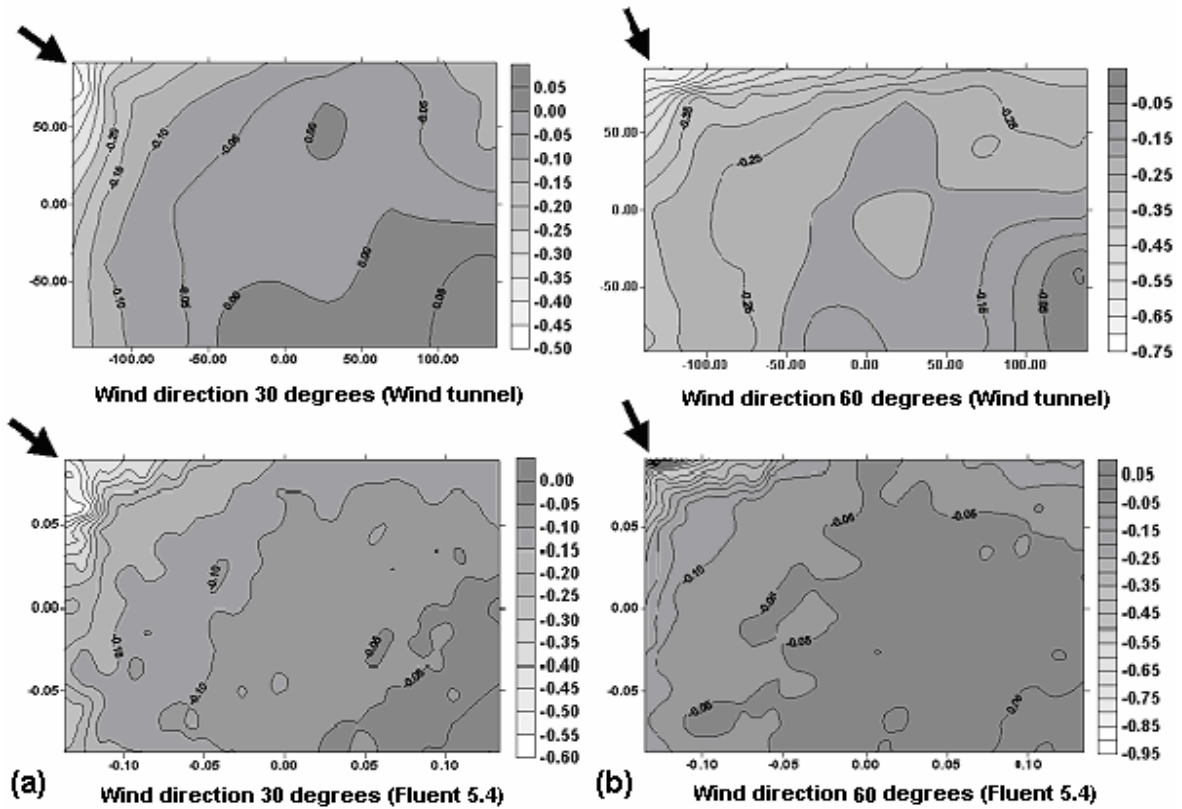
Figure 4. (a) Comparisons of mean pressure coefficients on the centerline of the roof for case N=1: experiments and numerical simulation using Fluent κ - ϵ model. (b) Comparisons of mean C_p on the centerline of the downwind wall of street canyon (or upwind wall of the downwind building) for case N=1: experiments and numerical simulation using Fluent κ - ϵ model

Figure 5a and 5b show comparisons of distributions of mean C_p on the roof for case N=1, B/H=1 at wind directions 30 and 60 degrees. Both of the graphs show similar trends with different angles of the approaching winds. The measured values of mean C_p are reasonably close to the calculated values. There is no root mean square (RMS) pressure coefficient provided from the output of Fluent, since Fluent is a steady-state Reynolds averaged model computer program. However, RMS pressure coefficients can be estimated from calculated mean pressure coefficients, mean velocities and RMS velocities using equations 6.1 and 6.2 proposed by Paterson [23]. Figure 6 shows RMS pressure coefficients plotted against mean pressure coefficients for roof pressure taps from wind tunnel results as predicted by Equations 6.1 and 6.2. Since the predictions of RMS pressure by both equations at the near zero mean pressure coefficients are expected to be poor, only the isolated roughness flow case (B/H=6) with highest magnitude of the mean pressure coefficient are compared here. There is a near linear relationship between $C_p(\text{RMS})$ and $C_p(\text{mean})$ in figure 6.51 for each set of data. The slope of the line of best fit is about -0.4 for the wind tunnel results, -0.21 for equation 6.1, and -0.43 for equation 6.2, respectively

$$C_p' = 2[k_1/3 + 0.816|\overline{C_p}| \overline{U_0} \sqrt{k_0}] / \overline{V}^2$$

$$C_p'^2 = 8k_0^2 / \overline{U_0}^4 + 8\overline{C_p}^2 \overline{U_0}^2 k_0 / (\overline{U_0}^2 + 2k_0 - 2k_1)^2$$

Where, C_p' is the RMS pressure coefficient, C_p is the mean pressure coefficient, V is a mean reference velocity, U is the mean velocity, and k is the turbulent kinetic energy



{ Can you replot these figures using the same scale ranges for each figure? The reviewer is correct that different shading for different contours is confusing. }

Figure 5. Comparison of distributions of mean C_p for case $N=1$, $B/H=1$ between measured and calculated (Fluent) at wind direction. (a) 30 degrees and (b) 60 degrees.

Two numerical models are presented to compare with wind tunnel results from flow over the urban street area (isolated roughness flow case). Both equations correctly predict an increase in RMS pressure coefficients with an increase in the magnitude of the mean pressure coefficient. The RMS pressure coefficients calculated from equation 6.2 are in much better agreement with the wind tunnel than those from equation 6.1.

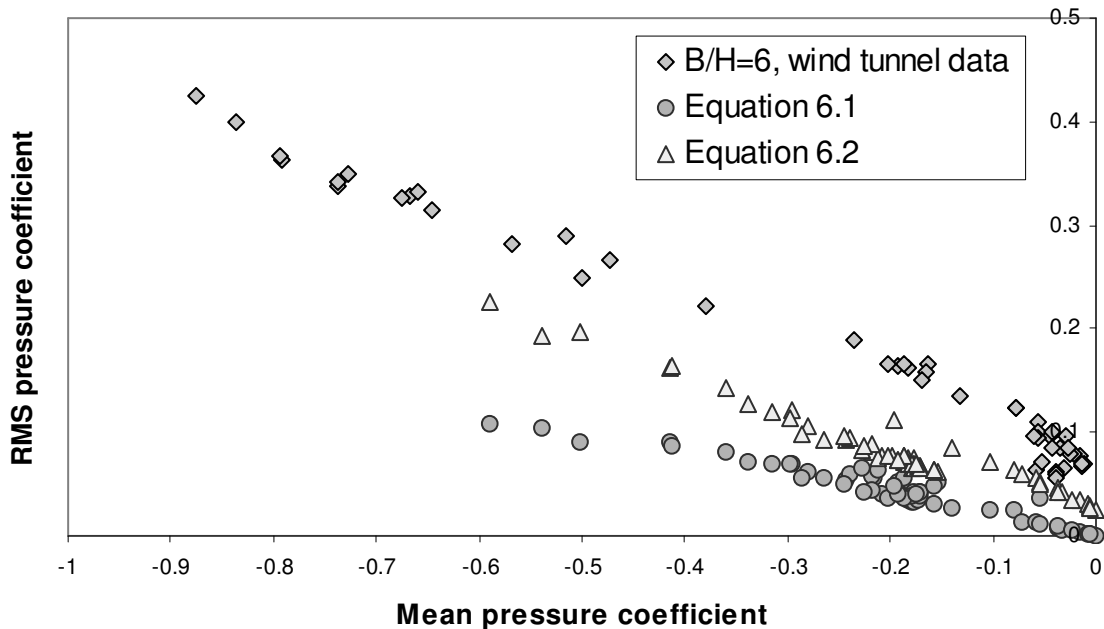


Figure 6 RMS vs. mean pressure coefficients form roof tapping, (B/H=6, N=1)

{In Figure 6 above can you move the scale to the left axis so it does not interfere with the data?}

4. CONCLUSION

The effects of surroundings significantly reduce the measured pressure coefficients, especially when the width of the street canyon is smaller (value of B/H is lower). For the same street canyon width, urban roughness cases tend to have greater shielding effects than the open-country cases. The suction on the roof can be significantly reduced by the presence of surrounding buildings. Compared to a single building case, building arrangements with B/H=0.5 can reduce the magnitude values of mean, RMS and –peak C_p 's over 80%.

The results of the comparison between numerical simulations and wind tunnel measurements show that it is not difficult to achieve similar trends in pressure behavior with spacing and orientation over a bluff body. However, it is not a given that quantitative equivalence between experimental and numerical data will occur unless careful attention is paid to inlet profiles, grid adaptation and the turbulent model chosen. In the calculation produced to replicate some of the test cases studied above, it was found necessary to take utmost care in adapting the turbulent grids to assure that separation locations and re-attachment locations were reproduced. Wind-tunnel flow and pressure tests performed about an idealized building arrangement replicate many of the features of the urban environment previously noted at full scale and in earlier laboratory simulations. Numerical simulations using Fluent reproduce these patterns, but only with care taken to provide adequate grid resolution, accurate inlet flow profiles, and improved turbulence models (for further details see Chang [22]).

ACKNOWLEDGEMENTS

The contribution of Dr. David E. Neff in coordinating and maintaining the experimental facilities and instrumentation in the Wind Engineering and Fluids Laboratory, CSU, is gratefully acknowledged. This work was supported by the US National Science Foundation through the CSU/TTU Cooperative Program in Wind Engineering, Grant No. CMS-9411147.

REFERENCE

- [1] Theurer, W. (1995). Point Sources in Urban Areas: Modeling of Neutral Gas Clouds with Semi-empirical Models, *Wind Climate in Cities*, Kluwer Academic Publishers, (Cermak et al., eds.) 485-502.
- [2] Banks, D. and Meroney, R. N., (1999). A model of roof-top surface pressure dependence upon local flow parameters, *Wind Engineering into the 21st century* (ed. Larsen, Larose & Livesey), Rotterdam: Balkema Press, 1097-1104.
- [3] Banks, D., Meroney, R. N., Sarkar, P. P., Zhao, Z. and Wu, F. (1999). Flow visualization of conical vortices on flat roofs with simultaneous surface pressure measurement, *Journal of Wind Engineering & Industrial Aerodynamics*, 27.
- [4] Plate, E. (2000). Wind loads and diffusion in urban areas, *Volume of Abstracts for 4th Int. Colloquium on Bluff Aerodynamics & Applications*, Ruhr-Universitat Bochum, Germany, September 11-14, 2000, Vol. 4, 3-7.
- [5] Surry, D. and Lin, J. X. (1993). The Effect of Surroundings and Roof Corner Geometric Modifications on Roof Pressures on Low-Rise Buildings, University of Western Ontario, Ontario, Canada, December 1993.
- [6] Kiefer, H. and Plate, E. J. (1998). Modeling of mean and fluctuating wind loads in built-up areas, *Journal of Wind Engineering and Industrial Aerodynamics*, Vol. 74-76, 619-629.
- [7] MacDonald, R. W. (2000). Modeling the Mean Velocity Profile in the Urban Canopy Layer, *Boundary-Layer Meteorology*, Vol. 97, 25-45.
- [8] He, J. and Song, C. C. S., (????) A numerical study of wind flow around the TTU building and the roof corner vortex, *Journal of Wind Engineering and Industrial Aerodynamics*, Vol. 67&68, 547-558.
- [9] Maruyama, T. and Maruyama, Y. (2000). Large eddy simulations around a rectangular prism using artificially generated turbulent flows, *Abstracts of papers at 3rd Int. Symposium on Computational Wind Engineering*, University of Birmingham, UK, September 4-7, 2000, 11-14.
- [10] Lee, S. (1997). Unsteady aerodynamic force prediction on a square cylinder using k- ϵ turbulence models, *J. of Wind Engineering and Industrial Aerodynamics*, Vol. 67&68, 79-90.
- [11] Selvam, R. P. (1997). Computation of pressures on Texas Tech University building using large eddy simulation, *Journal of Wind Engineering and Industrial Aerodynamics*, Vol. 67&68, 647-657.
- [12] Rehm, R. G., McGrattan, K. B., Baum, H. R. and Simiu, E. An Efficient Large Eddy Simulation Algorithm for Computational Wind Engineering: Application to Surface Pressure Computations on a Single Building, *NISTIR 6371*, Building and Fire Research Laboratory, NIST, Gaithersburg, MD. Website: <http://fire.nist.gov>.
- [13] Cheatham, S. A., Cybyk, B. Z. and Boris, J. P. (????) Simulation of Flow and Dispersion around a Surface-mounted Cube, Naval Research Laboratory, Washington, DC.
- [14] Carpenter, P. and Locke, N. (1999). Investigation of wind speeds over multiple two-dimensional hills, *Journal of Wind Engineering and Industrial Aerodynamics*, Vol. 83, 109-120.[15] Chang, C.H. and Meroney, R.N. (2000), Numerical and Physical Modeling of Bluff Body Flow and Dispersion in Urban Street Canyons, OF BLUFF BODY FLOW AND DISPERSION IN URBAN STREET CANYONS, *4th Int. Colloquium on Bluff Body Aerodynamics and Applications*, Ruhr-University, Bochum, Germany, 11-14 September 2000, 4 pp.
- [16] Chang, C.H. and Meroney, R.N. (2002), Concentration Distributions from a Point Source within Urban Street Canyons: Wind tunnel and Computational Data, Accepted for publication by *Boundary Layer Meteorology*, November 2002.
- [17] Cochrane, L. S. (1992). Wind-tunnel Modeling of Low-rise Structures. Ph.D. Dissertation, Department of Civil Engineering, Colorado State University, 348.

- [18] Birdsall, J. B. (1993). Physical Simulation of Wind-forced Natural Ventilation. Master Thesis, Department of Civil Engineering, Colorado State University.
- [19] Ham, H. J. (1998). Turbulence Effects on Wind-induced Building Pressures, Ph.D. Dissertation, Department of Civil Engineering, Colorado State University, 275.
- [20] Banks, D. (2000). The Suction Induced by Conical Vortices on Low-Rise Buildings with Flat Roofs. Ph.D. Thesis, Department of Civil Engineering, Colorado State University
- [21] Fluent 5: User's Guide, July 1998. Fluent Incorporated. Website: <http://www.fluent.com>.
- [22] Chang, H.C. (2001), *Numerical and physical modeling of bluff body flow and dispersion in urban street*, Ph.D Thesis, Department of Civil Engineering, Colorado State University, 242 pp. [23] Oke, T. R. (1998). Street design and urban canopy layer climate, *Energy and Buildings* 11, 103-113.
- [24] Paterson, D. A.(1992). Predicting r.m.s. pressures from computed velocity and mean pressures, *Journal of Wind Engineering and Industrial Aerodynamics*